Biochimica et Biophysica Acta 1827 (2013) 311–318

Contents lists available at SciVerse ScienceDirect

Biochimica et Biophysica Acta

journal homepage: www.elsevier.com/locate/bbabio

Allophycocyanin and phycocyanin crystal structures reveal facets of phycobilisome assembly

Ailie Marx, Noam Adir *

Schulich Faculty of Chemistry, Technion-Israel Institute of Technology, Haifa, 32000, Israel

ARTICLE INFO

Article history:
Received 27 September 2012
Received in revised form 12 November 2012
Accepted 16 November 2012
Available online 28 November 2012

Keywords:
Photosynthesis
Cyanobacterium
X-ray crystallography
Complex assembly
Urea

ABSTRACT

X-ray crystal structures of the isolated phycobiliprotein components of the phycobilisome have provided high resolution details to the description of this light harvesting complex at different levels of complexity and detail. The linker-independent assembly of trimers into hexamers in crystal lattices of previously determined structures has been observed in almost all of the phycocyanin (PC) and allophycocyanin (APC) structures available in the Protein Data Bank. In this paper we describe the X-ray crystal structures of PC and APC from *Synechococcus elongatus* sp. PCC 7942, PC from *Synechocystis* sp. PCC 6803 and PC from *Thermosynechococcus vulcanus* crystallized in the presence of urea. All five structures are highly similar to other PC and APC structures on the levels of subunits, monomers and trimers. The *Synechococcus* APC forms a unique loose hexamer that may show the structural requirements for core assembly and rod attachment. While the *Synechococcus* PC assembles into the canonical hexamer, it does not further assemble into rods. Unlike most PC structures, the *Synechocystis* PC fails to form hexamers. Addition of low concentrations of urea to *T. vulcanus* PC inhibits this proteins propensity to form hexamers, resulting in a crystal lattice composed of trimers. The molecular source of these differences in assembly and their relevance to the phycobilisome structure is discussed.

1. Introduction

The phycobilisome (PBS), found in cyanobacteria and red algae, is the largest photosynthetic antenna complex where individual co-factors are bound to the protein scaffold. PBSs are assembled from two sub-complexes, a central core with 2–5 cylinders surrounded by 6–8 rods [1–4]. These two sub-complexes are each built up from structurally similar pigmented phycobiliproteins (PBPs); allophycocyanin (APC, $\lambda_{max}=652$ nm) in the cores and phycocyanin (PC, $\lambda_{max}=620$ nm) in the rods (with additional pigmented components in some species absorbing in the 500–600 nm region) [3], and a variety of unpigmented proteins collectively called linker proteins (LPs) [5]. The different types of PBPs are highly similar in three dimensional structure and self associate analogously [6]: the basic monomer component (obtained spontaneously from the association of two homologous subunits called α and β) forms trimers which can then associate further into hexamers (mostly by interactions between α subunits). Rods are tube-like structures formed from association between hexamers (mostly by interactions between β subunits) while core cylinders contain four APC trimers in more loosely packed hexamers [7] with a similar trimer:trimer association [8–10]. LPs occupy the central cavities formed by the PBP discs and have been proposed to have a structural role in mediating the interactions between, or "linking", PBPs and also as having the ability to modify the spectral properties of the pigmented components [11,12]. LPs, the number of which varies from species to species, are grouped according to their position within the PBS complex — rod capping, rod, rod–core, core and core-membrane [5].

To date EM images have provided low resolution images of the overall PBS architecture and high resolution X-ray crystal structures have provided detail on the isolated components, particularly the PBPs. The largest PBS sub-structures for which crystal structures were obtained from an isolated complex of the same assembly size (and not due to further assembly *in crystal*) are the phycoerythrin (PE) hexamer from *Griffithsia monilis* (PDB id: 1B8D)[13] and the recently reported PC rod (containing two hexamers) from *Thermosynechococcus vulcanus* (PDB id: 3O2C) [11]. Both of these assemblies contained LPs, however in both cases the linkers were positioned along crystallographic symmetry axes resulting in an inability to clearly identify the linker position within the electron density maps. Given the tendency of the isolated PBP components (usually trimers) to associate *in crystal* into hexamers (and in some cases further into essentially infinite rods) in a fashion analogous to that presumed to occur *in vivo*, it is tempting to

Abbreviations: APC, allophycocyanin; LP, linker protein; PBP, phycobiliprotein; PBS, phycobilisome; PC, phycocyanin; PCB, phycocyanobilin; Se, *Synechococcus elongatus* sp. PCC 7942; Se_APC, *Synechococcus elongatus* sp. PCC 7942 allophycocyanin; Se_PC, *Synechococcus elongatus* sp. PCC 7942 phycocyanin; Sy, *Synechocystis* sp. PCC 6803; Sy_PC, *Synechocystis* sp. PCC 6803 phycocyanin; Tv, *Thermosynechococcus vulcanus*; Tv_PC, *Thermosynechococcus vulcanus* phycocyanin

* Corresponding author. Tel.: +972 4 8292141; fax: +972 4 8295703.
E-mail address: nadir@tx.technion.ac.il (N. Adir).

0005-2728/$ – see front matter © 2012 Elsevier B.V. All rights reserved.
http://dx.doi.org/10.1016/j.bbabio.2012.11.006

superimpose the high resolution details of higher orders of association in the crystal structures of individual PBP components onto lower resolution EM derived descriptions of the complex. However, since not all crystal structures form the same lattices, there have been additional proposals as to how hexamers and rods are formed [14]. The mode of assembly of trimers into hexamers and further into rods is functionally important, since it determines how each chromophore is positioned relative to its nearest neighbours (with respect to distance and angles) and thus determines the most probable pathways of energy transfer [15–17]. This aspect of PBS functionality becomes even more important when trying to assess how the rods are attached to the core. In some PBS models derived by EM studies, the rods are attached to the core in a mostly perpendicular fashion. This organization would also orient the rod cofactors (especially the α84 and β84 phycocyanobilins of PC) in a nearly perpendicular fashion with respect to the core APC cofactors. It has been shown that both inter-rod and rod–core energy transfer kinetics have extremely fast components [15], yet these two energy transfer steps should have vastly different geometries. To this extent, we must also address specialized PBS complexes such as those of *Gloeobacter violaceus* [17] and *Acaryochloris marina* [18,19] which also exhibit fast energy transfer from PC to APC.

All but one of the 20 PC structures in the PDB form hexamers from trimers *in crystal* [4,20]. The integrity of isolated PBS complex or rods or core substructures in solution requires the presence of high concentrations of phosphate buffer (0.5–0.9 M). For the vast majority of proteins, the intermolecular contacts and packing in the crystal lattice are notoriously affected by the crystallization process. However none of the hexamer forming PC structures required crystallization in the presence of high concentrations of phosphate buffer and the pH of the crystallization solutions range from 4.6 to 8.5 [1]. Interactions between PBP monomers are mostly hydrophobic in nature and the formation of a trimer leads to a buried surface area of about 500 $Å^2$ [1]. The trimer-trimer interface (leading to hexamer formation) contains mainly charged and polar interactions [1,21]. It is important to note that the entire PBS (including the already formed rods) disintegrates rapidly into trimers upon isolation in buffers lacking at least 0.5 M phosphate. Thus it appears that chemical forces that lead to assembly do not induce the formation of very strong intramolecular interactions. The limited stability of the PBS may have importance for the directed disassembly of the PBS *in vivo* when cells undergo nutrient stress [22,23].

If we assume that the propensity of PC to form hexamers is intrinsic and independent of outside components (linkers or chaperones), then the hexamers found *in crystal* are most likely representative of the biological hexamer. It then becomes important to try to address the question as to the source of the anomalous non-hexamer forming structures. Indeed the first PC structure solved, for PC isolated from *Mastigocladus laminosus*, was non-hexamer forming [24] although these coordinates were never deposited in the PDB and so further analysis on the structure cannot be carried out. The only non-hexamer forming PC structure in the PDB to date is one of several structures of PC isolated from the cyanobacterium *T. vulcanus*. The PC fraction from which crystals were grown was indeed unique, being unmethylated and processing a distinctive blue shifted absorption [20]. However these features or detailed structural analysis failed to explain the anomaly in crystal packing.

We present here five new crystal structures that exhibit different aspects of hexamer formation. The structures of APC and PC from *Synechococcus elongatus* sp. PCC 7942 (Se_APC and Se_PC, respectively) both form hexamers, however they exhibit significant, and perhaps functionally relevant differences in their higher order assembly. The structure of PC isolated from *Synechocystis* sp. PCC 6803 (Sy_PC) is only the second example of a PC structure with anomalous lattice packing whereby hexamers fail to form. Additionally we show that we can inhibit *T. vulcanus* PC (Tv_PC) hexamer formation by the addition of low concentrations of urea.

2. Materials and methods

2.1. Growth of cells and isolation of PBPs

Synechocystis sp. PCC 6803 (Sy) and *S. elongatus* sp. PCC 7942 (Se) cells were grown in 3 litre Erlenmeyer flasks on 1 litre of BG11 medium and were shaken at 30 °C with continuous fluorescent lamp illumination for 3–4 days before harvesting. Cells were collected by centrifugation, resuspended in protein isolation buffer (20 mM Tris,10 mM $MgCl_2$, and 10 mM $CaCl_2$, pH 8), and treated with lysozyme (1 mg/ml) for 1 hour on ice before passing through a Yeda press cell disrupter under 25 atm of N_2. Following 30 min of centrifugation at 10,000 rpm, the blue supernatant containing the different PBPs in their trimeric forms were first passed through a DEAE anion-exchange low-pressure liquid chromatography column to obtain partially purified fractions. These fractions were further purified by HPLC anion exchange chromatography as previously described [20]. Protein samples were concentrated by ultrafiltration using a Centricon 100 K (Amicon). PC from *T. vulcanus* (Tv) was analogously purified however cells were grown as 2 L in a 10 L cylinder at 55 °C and lysoyzme treatment was carried out at 55 °C. Purified PC was introduced to different concentrations of urea (2 M or 4 M) buffered with 20 mM Tris–HCl pH 8 after purification and prior to concentration.

2.2. Crystallization, data collection and structure determination

Sy_PC was crystallized in 6% PEG (polyethylene glycol) 4000, 400 mM MgSO4, and 20 mM Tris, pH 8, using the hanging-drop vapor diffusion technique at 20 °C. Cryoprotection in a mixture of 30% ethylene glycol and 70% crystallization reservoir was carried out by soaking prior to flash freezing. Se_PC was crystallized in 20% PEG 4000, 50 mM tris pH 8 and Se_APC was crystallized in 30% PEG 4000, 50 mM Tris pH8 and both were cryoprotected in silicon oil prior to flash freezing. PC from *T. vulcanus* in buffer containing 2 M, 3 M or 4 M urea was crystallized in 0.8 M $(NH_4)_2SO_4$ and 20 mM Tris pH8 (giving final concentrations of urea 1 M, 1.5 M and 2 M) using the hanging-drop vapor diffusion technique at 20 °C. 70% glucose was used to cryoprotect the crystals prior to flash freezing. Diffraction quality crystals were obtained for every concentration of urea. Data collection was carried out at the European Synchrotron Radiation Facility (ESRF) on beamlines ID23-1 and ID14-4. Data was scaled and merged using MOSFLM [25] and molecular replacement was carried out with Phaser [26]. The structures were refined using Crystallography & NMR System [27] interspersed with manual modifications of the model into calculated electron density and visualized using Coot [28]. Structural alignments were also carried out in Coot and structural visualization, surface electrostatic potentials, B-Factor analysis and structure figure preparation was performed using PyMOL [29].

2.3. Analysis of crystals by confocal microscopy

The fluorescence emission spectra from single crystals were obtained using an LSM 510 META laser scanning confocal microscope (Zeiss) with a DPSS laser with excitation line at 561 nm.

2.4. Accession numbers

Coordinates and structure factors have been deposited in the Protein Data Bank with the following accession numbers: Sy_PC: 4F0T; Se_PC: 4H0M; Se_APC: 4F0U, Tv_PC_4MU:4GXE and Tv_PC_2MU: 4GY3.

3. Results and discussion

3.1. The APC structure from S. elongatus sp. PCC 7942 may contain the L_C linker protein

The fresh water cyanobacterium *S. elongatus* sp. PCC 7942 (Se) is one of the few phycobilisome containing organisms that contain a bicylindrical core [30]. While Se is one of the most highly studied strains of cyanobacteria, no PBP crystal structures have been determined to date. We have isolated, and determined the structures of both Se_APC and Se_PC to resolutions of 2.5 Å and 2.2 Å, respectively (Table S1). Se_APC was isolated in trimeric form and crystallized in the $C2_12_12_1$ space group, which is unique when compared to other APC structures solved to date. The asymmetric unit also contains a trimer, which shows higher assembly into a hexamer. In assessing the similarity of this new structure to previous APC structures we found that the Se_APC trimer is more similar in overall structure to that of the core linker (L_C) containing *M. laminosus* 1B33 APC structure [31], than to APC structures that lack the L_C (an rmsd for all Cα atoms of 1.1 Å, compared to an rmsd of 1.9 Å to the L_C -less 1KN1 APC structure). In both the Se_APC and 1B33 structures, the trimers are slightly flatter with respect to APC trimers lacking the L_C linker. The extremely unusual crystal packing of the 1B33 structure, allowed for visualization of the linker protein in the electron density map but prevented exploration of the effect of the linker on higher orders of aggregation such as hexamers. In contrast, the Se_APC structure forms hexamers in the crystal lattice, but the three fold symmetry of the PBP prevents the detection of electron density resulting from the presence of the linker, as has previously been show for PBPs cocrystallized with linker proteins [11,13]. Analysis of the B-factors in the structure showed a variance between the three monomers forming an APC trimer. A small helix (formed by residues 115–122) and the β84 PCB of one of the three monomers, facing the inner cavity of the APC disk have elevated B-factors in comparison with the other two monomers (Fig. 1). This is interesting, considering that the L_C linker in the 1B33 structure was found to associate with two out of the three monomers in the trimer [31]. Presumably, interaction between the APC and L_C would stabilize and thus lower the B-factors of the residues in the interaction interface. If the linker in the Se_APC structure is similarly positioned close to two of the three monomers this would explain the lowered B factors in two of the three monomers at positions exposed to the central cavity of the APC trimer. The difference in the B-factor is not the result of crystal packing, as all three loops do not participate in lattice formation.

Only a very limited number of crystals were available for analysis. We thus wanted assess a single Se_APC crystal by fluorescence emission confocal microscopy which has a special resolution of 1 μm^3 (Fig. S1). The effect of the presence of the L_C within an APC trimer has previously been shown to be red shifted by 2 nm compared to that of pure APC [32,33]. We have previously shown for crystalline PC and PC in rods with linkers that the crystalline state imparts a 4 nm red-shift in the position of the maximal fluorescence peak [34]. The results of the fluorescence analysis of the Se_APC crystals show a variable emission maximum at 663–667 nm, depending on the position of the measurement. Compared to the solution peak at 660 nm, these measurements are not completely conclusive with respect to the presence of the small core linker associated with APC. However it can be stated with certainty that the crystals are devoid of the minor core terminal emitter components (APC^B or L_{CM}) that fluoresce at much longer wavelengths [35]. Similar confocal microscope measurements made on *Synechocystis* core crystals [36] clearly show the presence of the terminal emitters. This indicates that four out of the eight APC trimers found in the bicylindrical Se_APC core are not found in the crystal. Of the four remaining trimers, two bind L_C and two do not. It is certainly possible that some heterogeneity in the crystal exist, however there are enough APC + L_C trimers to impart the change in ring flatness, as indicated above.

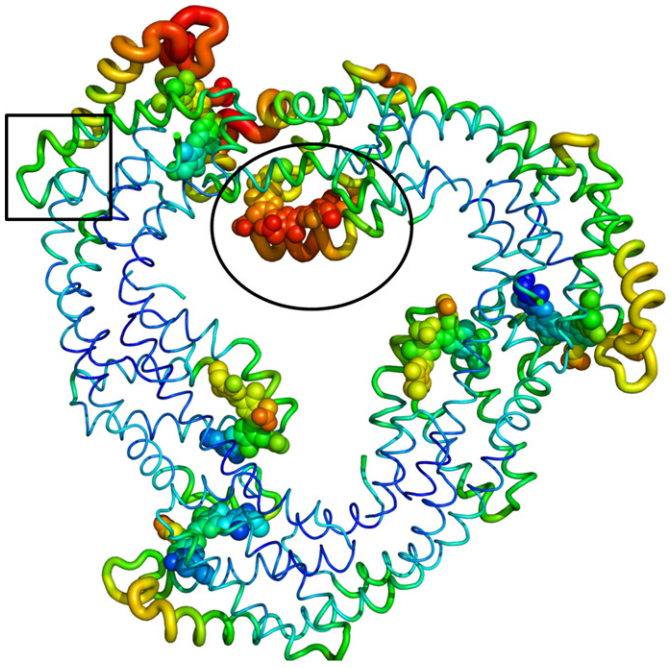

Fig. 1. One monomer in the trimer of Se_APC shows elevated B factors in regions exposed to the central cavity. The Se_APC structure is depicted and colored according to B factors (blue to red spectra and thin to thick tube width depicts increasing B-factor values). These values show that one of the small helices formed by residues 115–122 (black circle) that penetrates into the APC trimer void has elevated B factors with respect to the two other loops. The β84 PCB of the corresponding monomer also has elevated B factors (the three β84 PCB cofactors are shown in spheres and colored according to B factor). A black square indicates the position of the connecting loop between helices B and E on the α subunit.

3.2. The effect of the small core linker on the APC hexamer — a model for rod attachment to cores

It has been previously shown that deletion of the *apcC* gene, encoding for the L_C does not prevent the assembly of PBSs with nearly normal absorption and fluorescence emission properties [37]. However, the lack of L_C does lower PBS stability *in vitro*, and lowers the rate of cell division. Since the L_C is present in all PBS except those of *A. marina* (see below), what then is the role of the L_C? When visualized by utilizing the proper symmetry operator, the Se_APC hexamer is subtlety, but significantly different to those seen in either other APC structures or in PC structures. The association of the Se_APC trimers is through the α subunit faces, as is the case for all PC hexamers and also for the APC structures lacking L_C, *Porphyra yezoensis* 1KN1 and *G. violaceus* 2VJT. However in contrast to these structures where the outer circumference of the hexameric disc is tightly packed — in the Se_APC-L_C complex structure, a significant cavity is formed (Fig. 2). The result of this is that the gap between the loop region connecting helices B and E (Fig. 1; see Ref. [28] for nomenclature of PBP helices) between two adjacent monomers in the hexamer is widened creating three equivalent cavities in the outside circumference of the hexamer. These cavities are not the result of any special sequence difference with this region (residues 62–72 of the α subunit) since this portion of the sequence is completely conserved between the *P. yezoensis* APC and Se_APC and is highly conserved in all APC [38]. Strikingly, the outer circumference of this area of the 1KN1 hexamer is rather hydrophobic (Fig. 2B). In the Se_APC structure presented here, the opening of the long gap also reveals polar or charged residues further into the structure. These polar residues,

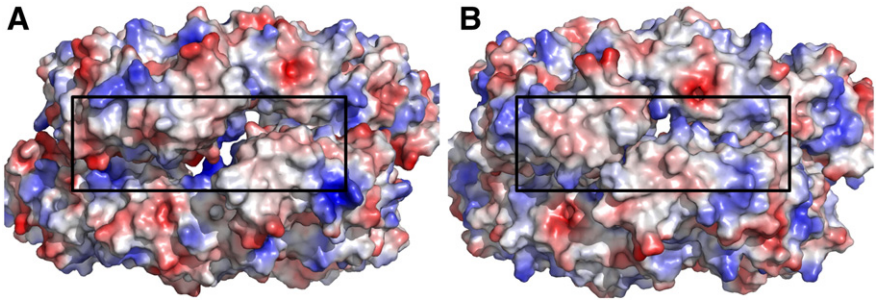

Fig. 2. The Se_APC structure reveals an aperture on the circumference of the hexamer. The hexameric molecular surfaces of Se_APC (A) and *P. yezoensis* APC (B, PDB: 1KN1) were calculated using Pymol. In both cases the hexamers are present in the crystal lattice although they were isolated as trimers. The surfaces are colored according to their relative vacuum electrostatic potential as calculated using the algorithm implemented in Pymol. Levels of blue and red indicate the approximate level of positive or negative potential, respectively. The black rectangles surround the cleft that is open in the Se_APC structure as compared to that of the 1KN1 structure.

lining the inside of the open gap may have a role in stabilizing the binding of the linking REP domains of the L_{CM} core membrane linker, proposed to stabilize the core structure [5,10] and/or the termini of the L_{RC} linkers suggested to link the rods to the cores. Concurrent with this suggestion, this type of opening is not required in the *A. marina* PBS. The *A. marina* PBS are composed of single rods lacking both the L_C and L_{CM} linkers, and the single APC trimer is attached directly (and not in a perpendicular fashion) to an adjacent PC trimer [39,40].

EM images have appeared to show a radial arrangement of the rods surrounding the core [41–44], however the interpretation of these images have led to different models, ranging from an almost equidistant (between rods) radial arrangement to three sets of parallel rod pairs [2,4,10]. The parallel rod model supports three distinct rod–core interactions. Indeed a structure of a functional PBS rod, containing all the associated linker proteins, rod capping, rod and rod–core, crystallized to give a PBP scaffold identical to that of isolated trimeric PC forms [11]. In this structure infinite rods were formed without the protrusion of the linker from the central cavity of PC however only one of the three different rod core linkers was detected in the crystals. Together this suggests that there may be different modes of association between different rods and the core. The controlling element may be the direction, and thus the availability, of the gap formed in the APC hexamer.

3.3. N-terminal cleavage of PC from S. elongatus PCC 7942 has no effect on assembly into hexamers

The first stage in the assembly of the PBS is the correct association of α and β subunits of the different PBPs. First identified by sequencing of the polypeptide [45], all crystal structures of APC to date have confirmed the absence of the N-terminal methionine residue of the α subunit. The mechanism for this cleavage has been suggested as the action of a methionyl-amino peptidases [46] which are known to cleave N-terminal methionines proceeding small side chain residues such as (G, A, S) and indeed the presence of such a small amino acid following the N terminal methionine is a conserved feature of the α chain of APC. Whilst such a feature has not been reported for other PBPs, some sequences of PC also contain this motif, among them Se_PC, where the N terminal methionine is followed by small amino acids on both the α and β chains [38]. We have determined the crystal structure of Se_PC to 2.2 Å (Table S1). This is the first PC with such a motif for which the structure has been solved and analysis of the electron density map of the PC structure from Se_PC indeed reveals the absence of the N terminal methionine from both the α and β chains of the mature protein (not shown). Alignment of the amino acid sequences for the α and β chains of Se_PC with that of PC from other species for which no such small amino acid is found adjacent to the N terminal methionine shows that the small amino acid is an insertion into the sequence — the *cpcA* and *cpcB* genes encoding for the α and β PC subunits of Se are one amino acid longer than usual for PC. Cleavage of the N terminal methionine thus results in an N terminal with the same length as for PC from other species for which there is no cleavage. Since PC has an extended N terminal with respect to APC (Fig. 3), it is not the end of the chain which is responsible for providing the correct electrostatics for monomer formation as in the case of APC. Whilst N-terminal cleavage is not a functionally crucial feature as with the α subunit of APC, it

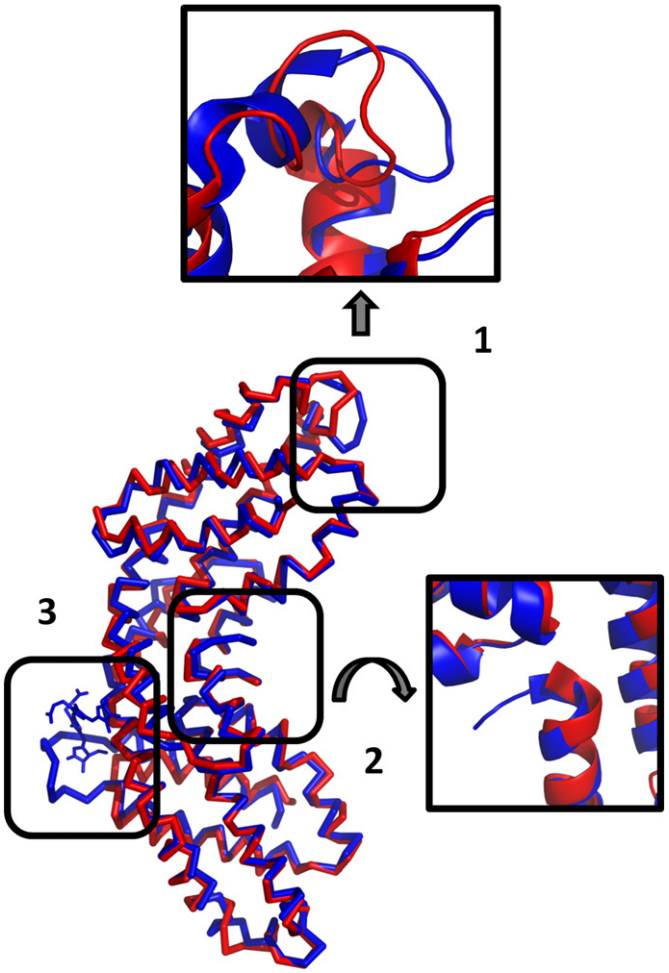

Fig. 3. Three major structural differences between the PC and APC monomer backbones. An alignment of PC (3O18, shown in blue) and APC (3DBJ, shown in red) shows three major structural difference highlighted in the insets: 1) the loop region between helices B and E is significantly variable; 2) PC has an extended N terminus compared to APC and 3) PC contains an extra loop which harbours the third PCB cofactor.

is apparently not detrimental either as long as the correct length of the N terminal chain is maintained.

Se_PC crystallized with 2 hexamers in the asymmetric unit which pack into layers of offset hexamers in a similar manner to the previously reported structures of PC isolated from *Phormidium* sp., *Spirulina* sp., and *Leptolyngbya* sp. [47–49]. Thus unlike the thermophilic Tv_PC, infinite rods are not formed *in crystal*. The hexamer-hexamer interactions seen in the Tv rod crystal structure (3O2C) has only a single polar interaction (not mediated by water molecules) between the Nε2 atom of βGln120 and the backbone carbonyl of the same residue on the symmetry related adjacent hexamer. This residue is a leucine in Se_PC and in *Spirulina* PC. This single change may be the major reason for successful rod formation *in crystal* (in the absence of linkers), although additional subtle changes may also provide additional stabilization.

3.4. Synechocystis sp. PCC 6803 PC does not form hexamers in the crystal lattice

PC from the mesophilic cyanobacterium Sy (Sy_PC) was isolated in its trimeric form and its structure was determined by X-ray crystallography to a resolution of 2.25 Å (Table S1). The asymmetric unit contains a monomer which is highly similar to previously determined PC structures from various species of cyanobacteria and red algae. The distinctive feature of the Sy_PC structure is the way in which trimers, also highly similar to previously determined PC structures, pack into the crystal lattice by a staggered association, primarily through the cofactor binding loop of the β subunit (Fig. 4). This arrangement is identical to that of the other nonhexamer forming PC structure from Tv (PDB id: 1ON7) [20], which was found to have a slightly blue shifted absorption maximum of 612 nm and lack methylation on the β72Asn residue — a hallmark of PBPs [50,51]. Sy_PC trimers however have the usual absorption characteristics (data not shown) and analysis of an omit map contoured onto β72Asn clearly confirms its methylation (Fig. S2) eliminating this as a factor directly affecting the aggregative state of PC. The question that arises is whether hexamer formation has been inhibited, and if so whether this is due to an intrinsic (sequence dependent) or extrinsic (crystallographic) property. Such an extrinsic property could either inhibit hexamer formation or promote the formation of layers of trimers in the crystal lattice.

Whilst the residues involved in trimer:trimer polar interactions are not absolutely conserved in all PCs [38], sequence comparison shows that Sy_PC contains the same residues identified as partaking in trimer:trimer interactions for a subset of the organisms which have been shown to produce hexamer forming PC structures. Artificial formation of a PC hexamer by superimposing two Sy_PC trimers onto a hexamer forming structure (PDB id: 3O18) shows only one apparent

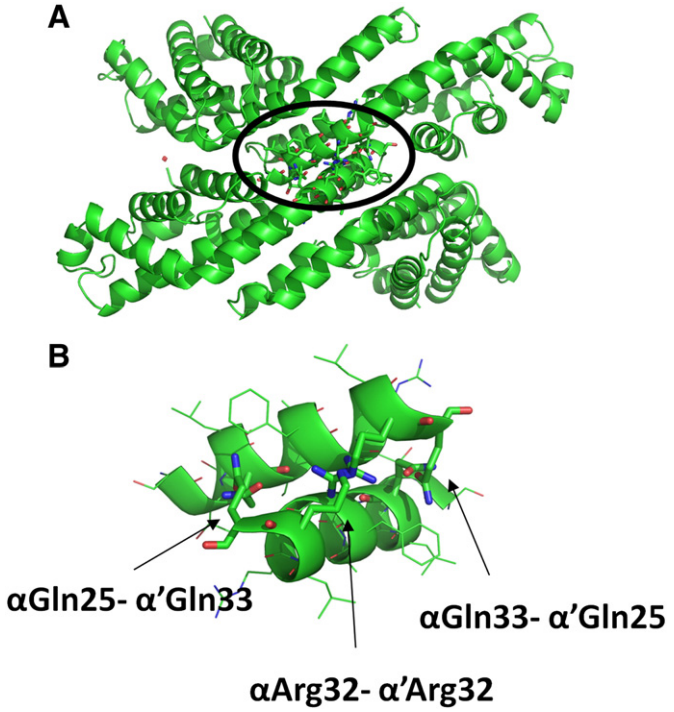

Fig. 5. Artificial formation of hexamers with the Sy_PC structure leads to three clashes between helices from adjacent α subunits. Panel A. Monomers from adjacent trimers in the artificially formed hexamer using the structure of PC from *Synechocystis* sp. *PCC 6803*. One monomer from each trimer is shown. The trimer–trimer interaction area where the clashes occur is circled in black. Panel B. Close up of circled area in panel A. The protein backbone is shown in cartoon representation. Residues which clash are highlighted as sticks and labelled, all other residues are in line representation.

impediment to the formation of hexamers. Three clashes occur between helices from adjacent α subunits that form close contact in the trimer-trimer interface of PC hexamers (Fig. 5). These residues, αArg32–α′Arg32, αGln25–α′Gln33 and αGln33–α′Gln25 (or chemically and sterically similar residues) are present in all species and are solvent exposed in the nonhexamer forming crystal type with no apparent special factor contributing to the orientation of these residues which would hold them in position thus preventing hexamer formation.

Analysis of the crystal structures of monomers from hexamer forming and nonhexamer forming PC structures reveals only one significant difference between the two forms — the distribution of B-factors. Whilst the B factors of the hexamer forming structures are

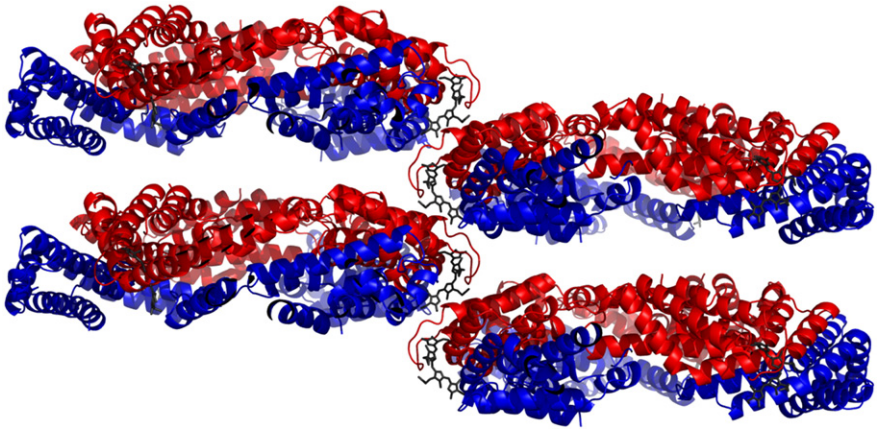

Fig. 4. Crystal packing of PC isolated from *Synechocystis* sp. *PCC 6803*. PC isolated from *Synechocystis* sp. *PCC 6803* crystallizes as columns of trimers (shown here from the side) separated by interpenetration by the adjacent column. PC is shown in cartoon representation with the α and β subunits colored in blue and red, respectively. The β155 PCB, which is involved in the crystal lattice formation, is shown as gray sticks.

relatively low and similar across the entire monomer (Fig. 6A), the B factors of the α subunit of the nonhexameric form are high relative to those of the β subunit (Fig. 6B). It would be reasonable to assume that this is a result of, rather than a determinant of, the crystal packing since the nonhexamer forming type of packing is looser and the α subunit is much more solvent exposed than in the hexamer forming type of packing. Surprisingly though, a similar analysis of APC structures, where trimers pack in different forms within the crystal lattice, shows relatively similar B factors across the structure regardless of the packing form, be it into hexamers or solvent exposed sheets of trimers (Fig. 6C).

Further analysis of the different PC structures (in the PDB and presented here) using the program PISA [52] was carried out. PISA calculates the most biologically relevant assembly out of those formed in crystal, based on chemical thermodynamics. For all PC structures, the hexameric assembly is indeed calculated by PISA as the most stable form (Table S2). Similar ΔG^{diss} values are obtained from structures in which the PC forms extended rods, or in other crystal packing forms. The stability of the trimers is markedly lower in most PC structures, however in the two non-hexamer structures (1ON7 and Sy_PC), the ΔG^{diss} values are higher (20 kcal/mol) as opposed to the hexamer forming PC (15.5 ± 4 kcal/mol). The PISA analysis might indicate a slight change in the overall PC trimer, too small to identify by visual inspection that prevents hexamer formation. Interestingly, a similar analysis for APC structures (Table S3) indicated that trimers are significantly more stable than hexamers. This indicates that the major source for hexamer stability in PC is the extra loop at the C-terminal end of β subunit, which binds the β155 PCB cofactor and wraps around the monomer below it in the hexamer. Even a small change in the position of this loop, or the presence of a small molecule impurity at this position might prevent hexamer assembly. To further investigate this prospect we set out to artificially disturb this association with forces outside the proteins intrinsic structure.

3.5. Monomerized PC reassembles into trimers but not hexamers in crystal

Lack of electron density associated with the presence of a disruptive compound in the non-hexamer forming PC crystal structures does not discount the presence of such a component since random association with the protein would prevent constructive interference of diffraction from these atoms. Some proteins, with an intrinsic propensity to crystallize, have been shown to also do so readily in the presence of high concentrations (up to 5 M in some cases) of urea [53]. We investigated whether the addition of such a chaotropic, hydrogen-bond forming (and thus also able to interfere with existing bonds) reagent could disturb the trimer:trimer interaction that is required for hexamer formation and is present in some PC crystal lattices. Purified Tv_PC was introduced into buffered solutions of urea to give final urea concentrations of 2.0 and 4.0 M urea. A shift in the λ_{max} of the PC sample in 4 M urea PC indicated that trimers had dissociated into monomers [2,3] (Fig. S3) and that dissociation was complete was demonstrated by the ability of the protein to pass through a 100 kDa ultrafiltration membrane. A significant amount of PC in the presence of 2 M urea remained in its trimeric form and was retained by the ultrafiltration membrane.

Monomeric PC from the 4 M urea treatment and trimeric PC in the presence of 2 M urea were then crystallized. In both cases, diffraction quality crystals were produced, in the $P6_3$ space group with lattice packing identical to that of the other non-hexamer forming

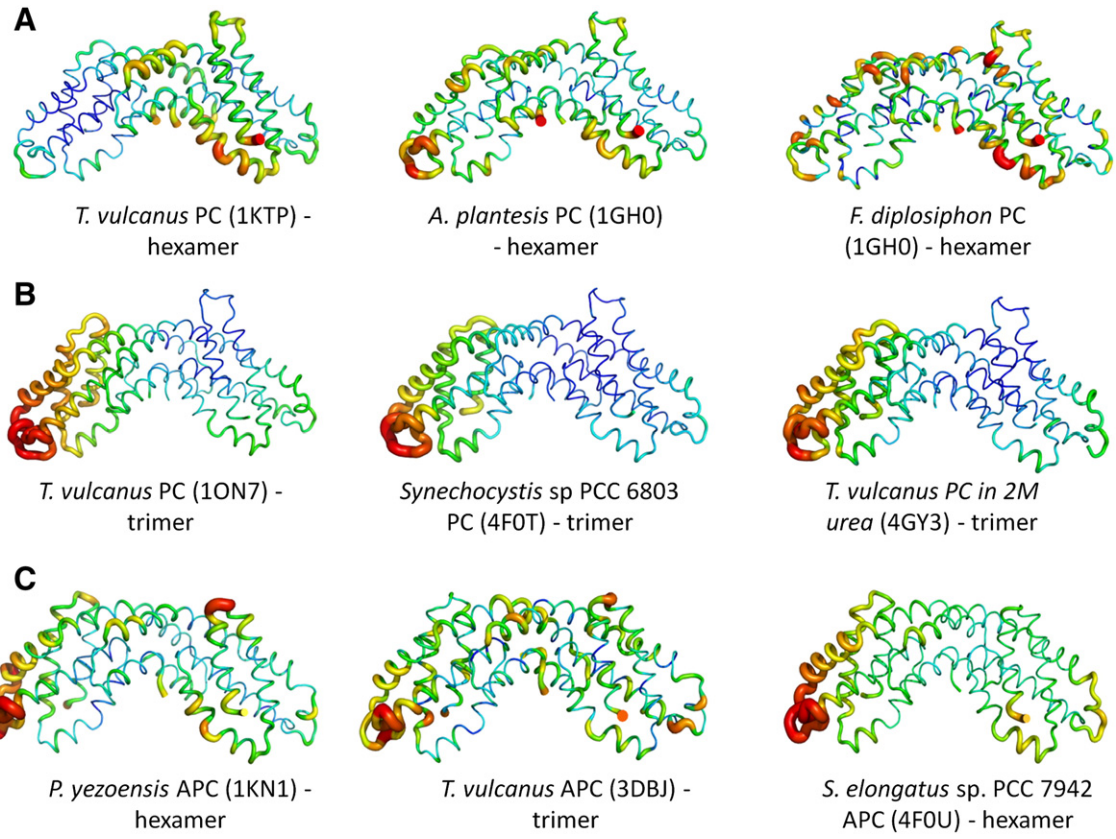

Fig. 6. B factors of nonhexamer forming PC but not APC structures are variable across the monomer. PC (panels A and B) or APC (panel C) structures are depicted by B-factor tubes as implemented in Pymol. All monomers are shown with the α and β subunits on the left and right side, respectively. Both the width of the tube and the blue to red gradation represents an increase in the relative magnitude of the B factors in each structure. Trimer or hexamer notation indicates the level of assembly in the crystal.

PC structures (Tv_PC_4MU, PDB id: 4GXE; Tv_PC_2MU, PDB id: 4GY3, respectively). This result indicates that PC monomerized by 4 M urea has the capability to reform trimers in the crystal lattice either as a result of the dilution of urea in the crystallization drop (to 2 M) or by the forces of crystallization, or by a combination of both. However it also shows that 2 M urea (1 M urea in the initial crystallization drop) is enough to prevent trimer-trimer association into hexamers *in crystal* (and further into rods). The structures were highly similar to all PC structures and analysis of the B-factor distribution showed a similar pattern of relatively high B-factors on the α subunit as was shown for the other non-hexamer forming PC structures (Fig. 6B).

The residues that interact to form hexamers in Tv_PC have been previously described [54,55]. It was proposed that a critical hydrogen-bond network between αAsp28, βAsn35, βPCB155 and α′Arg33 (PCB — phycocyanobilin cofactor; α′ is the α subunit of the second trimer in the hexamer) and specific water molecules stabilizes this level of assembly. The presence of urea could clearly weaken this critical interaction, leading to the alternative crystal packing. Close examination of the Tv_PC_2MU and Tv_PC_4MU structures show changes in the conformations of one the βPCB155 propionic acids that interacts with βAsn35. Two urea molecules bind close (but not directly) to this propionic acid (Fig. 7A). Even more dramatic is a shift in the orientation of the αArg33 side chain, critical for hexamer formation (Fig. 7B). In this position, not only does the αArg33 side chain not promote hexamer formation, it would clash with the α subunit of the second trimer, in a fashion similar to that seen in Fig. 5B for Sy_PC. Re-examination of the electron density map of the non-hexamer forming 1ON7 structure [20] shows that the αArg33 side chain has very weak density ($\sigma<1.0$) and probably should have been modelled in the non-hexamer forming conformation. B-factors in the non-hexamer Tv_PC structures indicate that the αArg33 side chain is flexible, and only upon hexamer formation is it locked into its alternate position. In both Tv_PC urea structures, a urea molecule is found bound in the vicinity of the αArg33 side chain, perhaps explaining its stabilization in this alternate position. We still do not have a clear explanation as to why the αArg33 side chain in the 1ON7 is shifted as compared to other Tv_PC structures. In the Sy_PC structure described above, the αAsp28 is replaced by a non-hydrogen bond forming phenylalanine, and thus formation of hexamers in the crystallization liquor may not be the preferred method of assembly, even in the absence of urea. However other PC structures lacking αAsp28 do form hexamers (such as 1CPC). Thus we can conclude that while hexamer formation *in crystal* appears to be the preferred level of assembly, the interactions between trimers in hexamer formation are quite weak, and can easily be disrupted by small molecules in the crystallization liquor.

In the Tv_PC_4MU structure, rings A, B and D of βPCB155 are moved out of the normal, very flat plane of the PCB. This may be a remnant of the urea treatment that lead to monomerization. A more complete description of the two Tv_PC structures obtained in the presence of urea will be given elsewhere.

4. Conclusions

In the five PBP structures presented here, we show how subtle are the interactions that lead to assembly, or non-assembly, of trimers into hexamers *in crystal*. In solution lacking stabilizing phosphate, trimers are the highest order assembly of PBPs and further stable assembly *in vivo* requires the presence of the linker proteins. The interaction interfaces between trimers are mostly polar, with only few potential hydrogen bonds. These are easily disrupted by even small changes in the structure as seen in the Sy_PC and Tv_PC_Urea structures. The intrinsic instability of the higher order assemblies is most likely the result of the need to disassemble the complex under conditions of stress. However our structures also show that slight difference in trimer structure can also result in major differences in the hexamer surface, which is most likely required for proper linker-dependent assembly. Our results reiterate the need for higher assembly crystal structures of the PBS that will show in what manner the linker proteins actually stabilize this complex and how the rods interact with the core cylinders.

Supplementary data to this article can be found online at http://dx.doi.org/10.1016/j.bbabio.2012.11.006.

Acknowledgments

This work was supported by the US–Israel Bi-National Science Foundation (2009406) and the Israel Science Foundation founded by the Israel Academy of Sciences and Humanities (1576/12). We gratefully thank the staff of the European Synchrotron Radiation Facility (beamlines ID-14-4, ID23-1) for provision of synchrotron radiation facilities and assistance. We thank Rakefet Schwarz and Gadi Schuster for providing us with *S. elongatus* sp. PCC 7942 and *Synechocystis* sp. PCC 6803 cells, respectively.

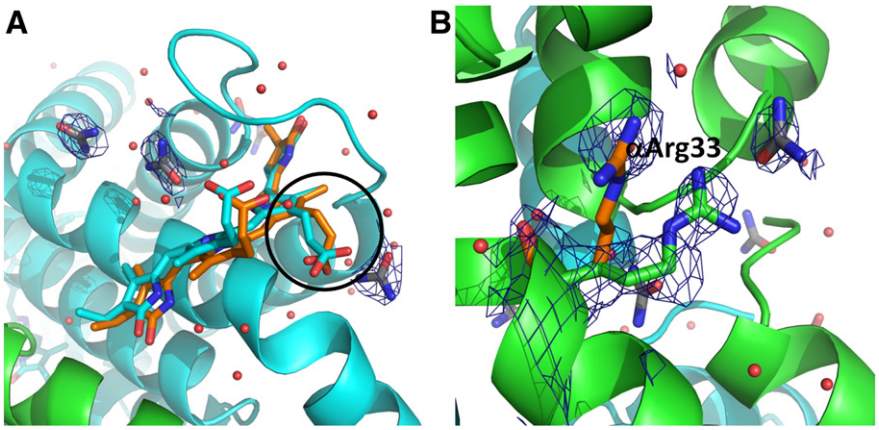

Fig. 7. *T. vulcanus* PC crystallizes as trimers in the presence of urea. Panel A. Propionic acid groups of βPCB155 in the Tv_PC_2M urea structure are shifted with respect to that of nonurea treated crystal structure 3O18 (orange carbons, only βPCB155 shown for clarity). The black circle denotes the propionic acid involved in hexamer formation. Panel B. Alternative position of αArg33 in the Tv_PC_2M urea structure (green carbons) as compared to a previously described PC structure in the absence of urea (3O18, orange carbons). A 2Fo–Fc electron density map is contoured at 1σ (blue mesh) onto the Arg residue from the Tv_PC_2M urea structure. Urea molecules identified in both panels are in stick representation with gray carbons and overlayed by a 2Fo–Fc electron density map contoured at 1σ.

References

[1] N. Adir, Elucidation of the molecular structures of components of the phycobilisome: reconstructing a giant, Photosynth. Res. 85 (2005) 15–32.
[2] A.N. Glazer, Light guides. Directional energy transfer in a photosynthetic antenna, J. Biol. Chem. 264 (1989) 1–4.
[3] R. MacColl, Cyanobacterial phycobilisomes, J. Struct. Biol. 124 (1998) 311–334.
[4] N. Adir, M. Dines, M. Klartag, A. McGregor, M. Melamed-Frank, Microbiology Monographs: Inclusions in Prokaryotes, in: J.M. Shively (Ed.), Springer, Berlin/Heidelberg, 2006, pp. 47–77.
[5] L.N. Liu, X.L. Chen, Y.Z. Zhang, B.C. Zhou, Characterization, structure and function of linker polypeptides in phycobilisomes of cyanobacteria and red algae: an overview, Biochim. Biophys. Acta 1708 (2005) 133–142.
[6] L.K. Anderson, C.M. Toole, A model for early events in the assembly pathway of cyanobacterial phycobilisomes, Mol. Microbiol. 30 (1998) 467–474.
[7] J.Y. Liu, T. Jiang, J.P. Zhang, D.C. Liang, Crystal structure of allophycocyanin from red algae *Porphyra yezoensis* at 2.2-A resolution, J. Biol. Chem. 274 (1999) 16945–16952.
[8] L.K. Anderson, F.A. Eiserling, Asymmetrical core structure in phycobilisomes of the cyanobacterium *Synechocystis* 6701, J. Mol. Biol. 191 (1986) 441–451.
[9] M. Glauser, D.A. Bryant, G. Frank, E. Wehrli, S.S. Rusconi, W. Sidler, H. Zuber, Phycobilisome structure in the cyanobacteria *Mastigocladus laminosus* and *Anabaena* sp. PCC 7120, Eur. J. Biochem. 205 (1992) 907–915.
[10] A. Ducret, S.A. Muller, K.N. Goldie, A. Hefti, W.A. Sidler, H. Zuber, A. Engel, Reconstitution, characterization and mass analysis of the pentacylindrical allophycocyanin core complex from the cyanobacterium *Anabaena* sp. PCC 7120, J. Mol. Biol. 278 (1998) 369–388.
[11] L. David, A. Marx, N. Adir, High-resolution crystal structures of trimeric and rod phycocyanin, J. Mol. Biol. 405 (2011) 201–213.
[12] D.J. Lundell, R.C. Williams, A.N. Glazer, Molecular architecture of a light-harvesting antenna. *In vitro* assembly of the rod substructures of *Synechococcus* 6301 phycobilisomes, J. Biol. Chem. 256 (1981) 3580–3592.
[13] S. Ritter, R.G. Hiller, P.M. Wrench, W. Welte, K. Diederichs, Crystal structure of a phycourobilin-containing phycoerythrin at 1.90-A resolution, J. Struct. Biol. 126 (1999) 86–97.
[14] B. Stec, R.F. Troxler, M.M. Teeter, Crystal structure of C-phycocyanin from *Cyanidium caldarium* provides a new perspective on phycobilisome assembly, Biophys. J. 76 (1999) 2912–2921.
[15] A.R. Holzwarth, Structure–function relationships and energy transfer in phycobiliprotein antennae, Physiol. Plant. 83 (1991) 518–528.
[16] A.R. Matamala, D.E. Almonacid, M.F. Figueroa, J. Martinez-Oyanedel, M.C. Bunster, A semiempirical approach to the intra-phycocyanin and inter-phycocyanin fluorescence resonance energy-transfer pathways in phycobilisomes, J. Comput. Chem. 28 (2007) 1200–1207.
[17] M. Yokono, S. Akimoto, K. Koyama, T. Tsuchiya, M. Mimuro, Energy transfer processes in *Gloeobacter violaceus* PCC 7421 that possesses phycobilisomes with a unique morphology, Biochim. Biophys. Acta 1777 (2008) 55–65.
[18] M. Chen, M. Floetenmeyer, T.S. Bibby, Supramolecular organization of phycobiliproteins in the chlorophyll d-containing cyanobacterium *Acaryochloris marina*, FEBS Lett. 583 (2009) 2535–2539.
[19] C. Theiss, F.J. Schmitt, J. Pieper, C. Nganou, M. Grehn, M. Vitali, R. Olliges, H.J. Eichler, H.J. Eckert, Excitation energy transfer in intact cells and in the phycobiliprotein antennae of the chlorophyll d containing cyanobacterium *Acaryochloris marina*, J. Plant Physiol. 168 (2011) 1473–1487.
[20] N. Adir, N. Lerner, The crystal structure of a novel unmethylated form of C-phycocyanin, a possible connector between cores and rods in phycobilisome, J. Biol. Chem. 278 (2003) 25926–25932.
[21] T. Schirmer, R. Huber, M. Schneider, W. Bode, M. Miller, M.L. Hackert, Crystal structure analysis and refinement at 2.5 A of hexameric C-phycocyanin from the cyanobacterium *Agmenellum quadruplicatum*. The molecular model and its implications for light-harvesting, J. Mol. Biol. 188 (1986) 651–676.
[22] J.L. Collier, A.R. Grossman, A small polypeptide triggers complete degradation of light-harvesting phycobiliproteins in nutrient-deprived cyanobacteria, EMBO J. 13 (1994) 1039–1047.
[23] M. Dines, E. Sendersky, L. David, R. Schwarz, N. Adir, Structural, functional, and mutational analysis of the NblA protein provides insight into possible modes of interaction with the phycobilisome, J. Biol. Chem. 283 (2008) 30330–30340.
[24] T. Schirmer, W. Bode, R. Huber, W. Sidler, H. Zuber, X-ray crystallographic structure of the light-harvesting biliprotein C-phycocyanin from the thermophilic cyanobacterium *Mastigocladus laminosus* and its resemblance to globin structures, J. Mol. Biol. 184 (1985) 257–277.
[25] A.G.W. Leslie, Recent Changes to the MOSFLM Package for Processing Film and Image Plate Data Joint CCP4 + ESF-EAMCB Newsletter on Protein Crystallography No. 26, 1992.
[26] A.J. McCoy, R.W. Grosse-Kunstleve, P.D. Adams, M.D. Winn, L.C. Storoni, R.J. Read, Phaser crystallographic software, J. Appl. Crystallogr. 40 (2007) 658–674.
[27] A.T. Brunger, P.D. Adams, G.M. Clore, W.L. DeLano, P. Gros, R.W. Grosse-Kunstleve, J.S. Jiang, J. Kuszewski, M. Nilges, N.S. Pannu, R.J. Read, L.M. Rice, T. Simonson, G.L. Warren, Crystallography & NMR system: a new software suite for macromolecular structure determination, Acta Crystallogr. D: Biol. Crystallogr. 54 (1998) 905–921.
[28] P. Emsley, K. Cowtan, Coot: model-building tools for molecular graphics, Acta Crystallogr. D: Biol. Crystallogr. 60 (2004) 2126–2132.
[29] W.L. DeLano, The PyMOL Molecular Graphics System, http://www.pymol.org 2002.
[30] G. Yamanaka, A.N. Glazer, R.C. Williams, Molecular architecture of a light-harvesting antenna. Comparison of wild type and mutant Synechococcus 6301 phycobilisomes, J. Biol. Chem. 255 (1980) 11104–11110.
[31] W. Reuter, G. Wiegand, R. Huber, M.E. Than, Structural analysis at 2.2 A of orthorhombic crystals presents the asymmetry of the allophycocyanin-linker complex, AP.LC7.8, from phycobilisomes of *Mastigocladus laminosus*, Proc. Natl. Acad. Sci. U. S. A. 96 (1999) 1363–1368.
[32] W. Reuter, W. Wehrmeyer, Core substructure in *Mastigocladus laminosus* phycobilisomes.1. Microheterogeneity in 2 of 3 allophycocyanin core complexes, Arch. Microbiol. 150 (1988) 534–540.
[33] L. Gottschalk, F. Lottspeich, H. Scheer, Reconstitution of allophycocyanin from *Mastigocladus laminosus* with isolated linker polypeptide, Photochem. Photobiol. 58 (1993) 761–767.
[34] L. David, A. Marx, N. Adir, High-Resolution Crystal Structures of Trimeric and Rod Phycocyanin, J Mol Biol. 405 (2011) 201–213.
[35] R. MacColl, Allophycocyanin and energy transfer, Biochim. Biophys. Acta 1657 (2004) 73–81.
[36] L. David, in Chemistry, Vol. Ph.D, Technion, Haifa, 2012.
[37] P. Maxson, K. Sauer, J.H. Zhou, D.A. Bryant, A.N. Glazer, Spectroscopic studies of cyanobacterial phycobilisomes lacking core polypeptides, Biochim. Biophys. Acta 977 (1989) 40–51.
[38] K.E. Apt, J.L. Collier, A.R. Grossman, Evolution of the phycobiliproteins, J. Mol. Biol. 248 (1995) 79–96.
[39] A.M. Collins, M. Liberton, H.D. Jones, O.F. Garcia, H.B. Pakrasi, J.A. Timlin, Photosynthetic pigment localization and thylakoid membrane morphology are altered in *Synechocystis* 6803 phycobilisome mutants, Plant Physiol. 158 (2012) 1600–1609.
[40] W. Swingley, R. Blankenship, J. Raymond, The Cyanobacteria: Molecular Biology, Genomic and Evolution, in: A.a.F., E. Herrero (Ed.), Caister Academic Press, Norfolk, U.K., 2008, pp. 21–44.
[41] E. Gantt, C.A. Lipschultz, Phycobilisomes of *Porphyridium cruentum*. I. Isolation, J. Cell Biol. 54 (1972) 313–324.
[42] A.N. Glazer, D.J. Lundell, G. Yamanaka, R.C. Williams, The structure of a "simple" phycobilisome, Ann. Microbiol. (Paris) 134B (1983) 159–180.
[43] A.A. Arteni, G. Ajlani, E.J. Boekema, Structural organisation of phycobilisomes from *Synechocystis* sp. strain PCC6803 and their interaction with the membrane, Biochim. Biophys. Acta 1787 (2009) 272–279.
[44] Z.W. Yi, H. Huang, T.Y. Kuang, S.F. Sui, Three-dimensional architecture of phycobilisomes from *Nostoc flagelliforme* revealed by single particle electron microscopy, FEBS Lett. 579 (2005) 3569–3573.
[45] W. Sidler, J. Gysi, E. Isker, H. Zuber, The complete amino acid sequence of both subunits of allophycocyanin, a light harvesting protein-pigment complex from the cyanobacterium *Mastigocladus laminosus*, Hoppe Seylers Z. Physiol. Chem. 362 (1981) 611–628.
[46] B. Datta, MAPs and POEP of the roads from prokaryotic to eukaryotic kingdoms, Biochimie 82 (2000) 95–107.
[47] X.Q. Wang, L.N. Li, W.R. Chang, J.P. Zhang, L.L. Gui, B.J. Guo, D.C. Liang, Structure of C-phycocyanin from *Spirulina platensis* at 2.2 A resolution: a novel monoclinic crystal form for phycobiliproteins in phycobilisomes, Acta Crystallogr. D: Biol. Crystallogr. 57 (2001) 784–792.
[48] A.K. Padyana, V.B. Bhat, K.M. Madyastha, K.R. Rajashankar, S. Ramakumar, Crystal structure of a light-harvesting protein C-phycocyanin from *Spirulina platensis*, Biochem. Biophys. Res. Commun. 282 (2001) 893–898.
[49] L. Satyanarayana, C.G. Suresh, A. Patel, S. Mishra, P.K. Ghosh, X-ray crystallographic studies on C-phycocyanins from cyanobacteria from different habitats: marine and freshwater, Acta Crystallogr. Sect. F Struct. Biol. Cryst. Commun. 61 (2005) 844–847.
[50] A.V. Klotz, J.A. Leary, A.N. Glazer, Post-translational methylation of asparaginyl residues. Identification of beta-71 gamma-N-methylasparagine in allophycocyanin, J. Biol. Chem. 261 (1986) 15891–15894.
[51] G. Shen, H.S. Leonard, W.M. Schluchter, D.A. Bryant, CpcM posttranslationally methylates asparagine-71/72 of phycobiliprotein beta subunits in *Synechococcus* sp. strain PCC 7002 and *Synechocystis* sp. strain PCC 6803, J. Bacteriol. 190 (2008) 4808–4817.
[52] E. Krissinel, K. Henrick, Inference of macromolecular assemblies from crystalline state, J. Mol. Biol. 372 (2007) 774–797.
[53] A.C. Pike, K.R. Acharya, A structural basis for the interaction of urea with lysozyme, Protein Sci. 3 (1994) 706–710.
[54] N. Adir, Y. Dobrovetsky, N. Lerner, Structure of C-phycocyanin from the thermophilic cyanobacterium *Synechococcus vulcanus* at 2.5 A: structural implications for thermal stability in phycobilisome assembly, J. Mol. Biol. 313 (2001) 71–81.
[55] N. Adir, R. Vainer, N. Lerner, Refined structure of C-phycocyanin from the cyanobacterium *Synechococcus vulcanus* at 1.6 A: insights into the role of solvent molecules in thermal stability and co-factor structure, Biochim. Biophys. Acta 1556 (2002) 168–174.